# Blume-Emery-Griffiths model on three-dimensional lattices: Consequences for the antiferromagnetic Potts model

Saulius Lapinskas* and Anders Rosengren
*Department of Theoretical Physics, Royal Institute of Technology, S-100 44 Stockholm, Sweden*
(Received 19 November 1993)

Using the cluster-variation method we study the phase diagram of the Blume-Emery-Griffiths (BEG) model on simple-cubic and face-centered cubic lattices. For the simple-cubic lattice the main attention is paid to reentrant phenomena and ferrimagnetic phases occurring in a certain range of coupling constants. The results are in close agreement with Monte Carlo data, available for parts of the phase diagram. Several ferrimagnetic phases are obtained in the vicinity of the line in parameter space, at which the model reduces to the antiferromagnetic three-state Potts model. Our results imply the existence of *three* phase transitions in the antiferromagnetic Potts model on the simple-cubic lattice. The phase diagrams for the BEG model on the face-centered cubic lattice are obtained in the region of antiquadrupolar ordering. Also the several ordered phases of the antiferromagnetic Potts model on this lattice are discussed.

## I. INTRODUCTION

The Blume-Emery-Griffiths (BEG) model is a spin-1 Ising model with up-down symmetry. This model is suitable for describing simple classical lattice systems with both density and symmetry-breaking degrees of freedom. Initially introduced to describe phase separation and superfluid ordering in $He^3$-$He^4$ mixtures,[1] the model was later applied to a number of systems including multicomponent fluids, microemulsions, semiconductor alloys, and electronic conduction models.

The Hamiltonian of the BEG model is

$$\mathcal{H} = -J\sum_{\langle ij\rangle} s_i s_j - K\sum_{\langle ij\rangle} s_i^2 s_j^2 + \Delta\sum_i s_i^2, \qquad (1)$$

where $s_i = 0, \pm 1$, and $\langle ij\rangle$ indicates summation over nearest-neighbor pairs.

The properties of the BEG model with $J + K > 0$, $J > 0$ are well established by extensive studies by means of mean-field approximations (MFA),[1–4] renormalization group techniques,[5] series expansion methods,[6] and by Monte Carlo (MC) methods.[7–10] Some exact results for the two-dimensional honeycomb lattice have been obtained for a limited subspace of the parameters $J$, $K$, and $\Delta$.[11–14] Some studies have been made also in the region $J + K > 0$ for bipartite lattices. A new staggered quadrupolar phase (also often called the antiquadrupolar phase) was predicted and investigated by means of MFA (Ref. 8) and MC simulation.[10] In this phase, $s_i = 0$ on one sublattice and $s_i = \pm 1$ at random on another. However different methods of investigation give a different global phase diagram so, e.g., while the mean-field approximation predicts reentrant phenomena for both ferromagnetic (F) and antiquadrupolar (A) phases, and a first-order phase transition (PT) between these two,[8] the renormalization group[15,16] (RG) and MC results point out that for the square lattice the A and F phases are always separated by the disordered phase and meet only at $T = 0$. The same result was obtained for the honeycomb lattice by the cluster-variation method (CVM).[17] Thus, the MFA results are apparently not valid for the *two-dimensional* lattices and the complete phase diagram for the BEG model on a two-dimensional bipartite lattice consists of three phases: paramagnetic (P), ferromagnetic, and antiquadrupolar.

The very rich phase diagram obtained by MFA (Refs. 18 and 19) featuring single- and double-reentrancy regions and ferrimagnetic phases for $K/J < -1$ could still be correct for *three-dimensional bipartite* lattices. Though the RG studies for $d$=3.05 did not obtain reentrancy and ferrimagnetic phases, it was suggested that this was a result of the restricted flow space, and the MFA result was assumed to be correct.[20] This assumption was confirmed by MC calculations showing the occurence of the double-reentrant F phase for $K/J \geq -1$ and $\Delta/J \geq 0$ (Refs. 21 and 22) and a ferrimagnetic phase.[21] A very recent RG analysis[15] also confirmed the MFA predictions for $d$=3. The accuracy of the MFA increases with increasing coordination number of the lattice, nevertheless a correct description of the ordering in *degenerate* systems may require a treatment of the short-range correlations which is beyond the capability of the MFA. Recently we applied the CVM analysis to the simple-cubic (sc) lattice and obtained some remarkable differences from the previous MFA results, concerning the locus $K/J = -3, \Delta/J = -12$, where the BEG model reduces to the antiferromagnetic Potts model. The complicated phase diagram unexpectedly predicts a sequence of *three* phase transitions for this model.[23]

Furthermore, the face-centered cubic (fcc) lattice, the lattice with the largest coordination number ($z = 12$), is not described by the results[19] when antiferromagnetic or antiquadrupolar ordering is in question since this lattice is not bipartite, i.e., cannot be divided to two interpenetrating sublattices with no nearest neighbors (NN) belonging to the same sublattice. Instead, to have no NN belong to the same sublattice four sublattices are needed. Thus, the fcc lattice is frustrated with respect to spin-$\frac{1}{2}$

 

and spin-1 Ising models in the presence of antiferromagnetic interactions. The BEG model on the fcc lattice has not been investigated so far, though it should be informative for the thermodynamics of ternary alloys and magnetic mixtures. It also seems interesting to investigate the properties of the three-state antiferromagnetic Potts model on the fcc lattice. Due to frustration, the ground state is also infinitely degenerate as in the sc lattice (the number of states is different from the number of sublattices) and it is reasonable to expect some odd behavior in this case too.

Here we present the results of CVM calculations for the BEG model on the simple-cubic lattice and show some qualitative differences from the previous MFA results[19] which where not covered by our previous work.[23] Further we investigate the phase diagram of the BEG model on the fcc lattice for $K/J < -1$, where antiquadrupolar ordering occurs. As a special case, the ordering of the antiferromagnetic Potts model on the fcc lattice is discussed in detail.

## II. SIMPLE-CUBIC LATTICE

The two-sublattice phase of the BEG model can be characterized by the magnetization and quadrupolar moment of sublattices $a$ and $b$:

$$m_a = \langle s_a \rangle\,,\ m_b = \langle s_b \rangle\,,\ q_a = \langle s_a^2 \rangle\,,\ q_b = \langle s_b^2 \rangle\,. \tag{2}$$

The values of these parameters define four phases with different symmetry. These are (1) paramagnetic phase (P) with $m_a = m_b = 0$, $q_a = q_b$, (2) ferromagnetic phase (F) with $m_a = m_b \neq 0$, $q_a = q_b$, (3) antiquadrupolar phase (A) with $m_a = m_b = 0$, $q_a \neq q_b$, (4) ferrimagnetic phase (I) with $m_a \neq m_b \neq 0$, $q_a \neq q_b$.

In the following consideration we put $J = 1$, so that one should think of temperatures and energies as normalized by $|J|$, where not stated otherwise. The $J < 0$ case can be mapped exactly on the $J > 0$ by redefining the spin direction for one sublattice of the bipartite lattice.

At $T = 0$ the perfectly ordered phases P, F, and A are separated by straight lines in the space $(K, \Delta)$:

$$\begin{aligned} &\Delta = 3(K+1)/2\,, \\ &\Delta = 0\,, \\ &\Delta = 3(K+1)\,, \end{aligned} \tag{3}$$

which are obtained by comparing the ground-state energies of the three phases.

The finite temperature phase diagram was calculated by the CVM in the eight-point "cubic" approximation. The details of the CVM for the BEG model are given elsewhere,[17] the only difference now being the set of clusters in the free-energy expansion. For the sc lattice we have used

$$F = F_8 - 3F_4 + 3F_2 - F_1, \tag{4}$$

where $F_8$, $F_4$, $F_2$, and $F_1$ are the free energies of the cube, square, nearest-neighbor pair, and single-site clusters, respectively. The cluster free energies $F_i$ depend on a set of variational parameters, which are obtained by the minimization of the total free energy under the self-consistency constraints. The total free energy can have several local minima, corresponding to different phases. We obtain the first-order phase transition lines by matching the free energies of the different phases, and the second-order lines are detected from the vanishing of order parameters (or the divergence of the corresponding susceptibilities).

The main attention in our investigation was paid to the reentrant phenomena and the occurrence of the ferrimagnetic phase. Here representative phase diagrams, relevant to these phenomena, are shown in Fig. 1. The reentrant and double-reentrant behavior is shown for $K = -0.5$ in the $(T, \Delta)$ plot in Fig. 1(a). Double reentrancy occurs in the region $1.46 < \Delta < 1.5$ and single reentrancy in the range $1.5 < \Delta < 1.51$. The second-order phase boundary is close to the result of the Monte Carlo renormalization group (MCRG) calculation[21] except that the range of the single reentrancy in MCRG is much more narrow, $1.5 < \Delta < 1.501$. But it is even qualitatively different from the MFA prediction[19] and recent RG results,[15] showing no critical point inside the F phase. We find that the critical line simply transforms to a first-order line at the tricritical point. Probably for $K$ closer to $-1$ the phase diagram will transform to that obtained by MFA at $K = -0.5$. In contrast to MCRG, we have obtained the location of the first-order transition line, corresponding to the multiphase equilibrium between the F and P phases.

The phase diagram at $K = -1.5$ obtained by the CVM [Fig. 1(b)] is qualitatively similar to the MFA result, and quantitatively close to the MCRG calculations. The appearance of a ferrimagnetic phase at low temperature near the first-order line between the F and A phases is shown in the inset. The phase is much more narrow than the MFA estimates (the lower-$\Delta$ limit being $-3.01$ for CVM and $-3.3$ for MFA). The MCRG predicts the value $\sim -3.006$.

The phase diagram for $K = -3$ is of particular interest, since the line $\Delta = -12$ (or, to be precise, its $J < 0$ counterpart) corresponds to the three-state antiferromagnetic Potts model with the Hamiltonian

$$\mathcal{H} = -2J \sum_{\langle ij \rangle} \delta_{s_i s_j}. \tag{5}$$

The ordered phase of this model is sixfold degenerate, and it was suggested[19] that these six phases should be accommodated in the BEG model by the first-order line meeting the twofold degenerate A phase and the fourfold degenerate I phase. The I phase was readily obtained in the MFA (Ref. 19) in the region $-13 > \Delta > -12$. No evaluation of the phase diagram at $K = -3$ was made by MC calculation. Our CVM analysis gives a much more narrow region of existence for the low-temperature ferrimagnetic phase $-12.05 > \Delta > -12$ which even cannot be distinguished on the scale of Fig. 1(c). The enlarged part of the phase diagram close to $\Delta = -12$, presented in the inset of Fig. 1(c), reveals quite an odd new topology—

actually two different ferrimagnetic phases do exist: one ($I_1$) corresponds to that obtained by the MFA and is a result of instability of the ferromagnetic phase against the two-sublattice ordering, another one ($I_2$) is caused by the instability of the A phase against spontaneous magnetization. Thus, in the higher-temperature region $1.574 < T < 2.535$ the sixfold degeneracy is obtained by coexistence of the twofold degenerate F phase and the fourfold degenerate ferrimagnetic $I_2$ phase. At lower temperature, $0 < T < 1.543$, the phase diagram is qualitatively similar to the MFA result.[19] The value of the

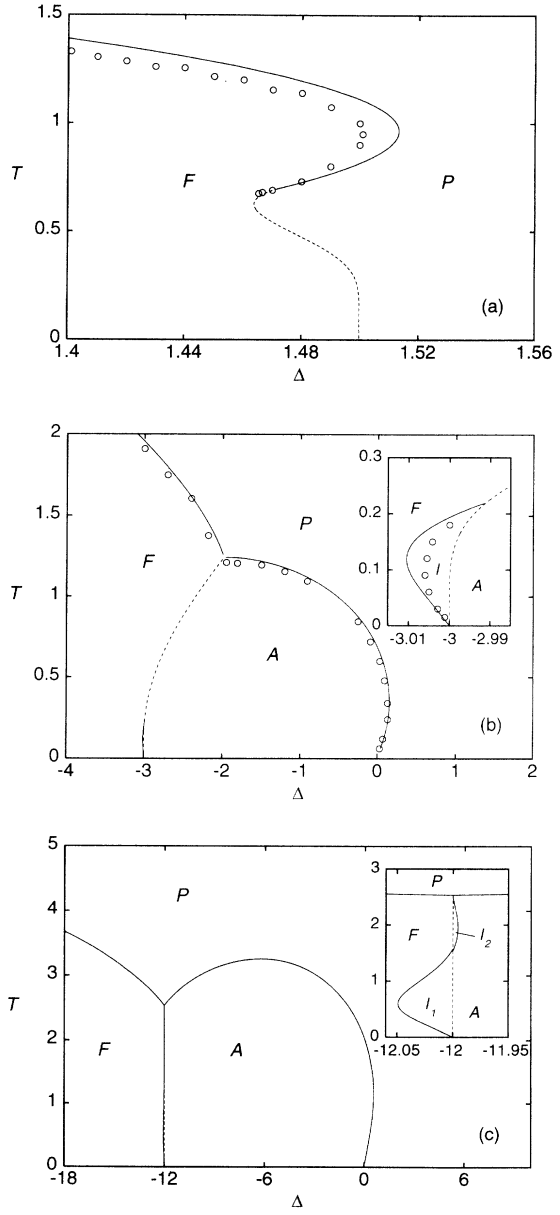


FIG. 1. Calculated $(T, \Delta)$ phase diagram of the BEG model at (a) $K = -0.5$, (b) $K = -1.5$, (c), $K = -3$. The solid and dotted lines represent the second- and first-order phase-transition lines, respectively, obtained by the CVM, the circles — MCRG results (Ref. 21). The temperature and the parameters $K$ and $\Delta$ are normalized by $|J|$.

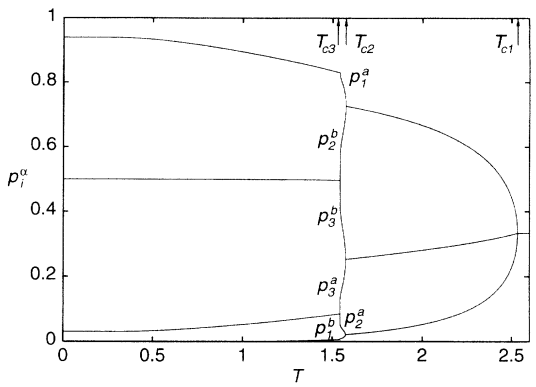


FIG. 2. The temperature dependence of the expectation values for different states of the AF Potts model, corresponding to $K = -3$ and $\Delta = -12$.

Potts transition $T_{c1} = 2.535$ is only 2.4% above the MC estimate[24] $T_c = 2.47 \pm 0.01$.

The appearance of the two ferrimagnetic phases is a rather unexpected result because it implies the existence of additional phase transitions in the ordered phase of the three-state antiferromagnetic Potts model on the sc lattice. Two additional phase transitions of the second- and first-order, respectively, separate regions with different types of ordering. These are described in detail in our previous work.[23] Here we only reproduce in Fig. 2 the temperature dependencies of the expectation values $p_i^\alpha$ of the three Potts states $i = 1, 2, 3$ on the two sublattices $\alpha = a, b$ in order to compare later with the corresponding results for the fcc lattice, results which appear to be very different. The equations

$$p_1^\alpha = \frac{1}{2}(q_\alpha - m_\alpha), \quad p_2^\alpha = 1 - q_\alpha, \quad p_3^\alpha = \frac{1}{2}(q_\alpha + m_\alpha) \tag{6}$$

relate these expectation values to the magnetizations and quadrupolar moments [Eq. (2)].

## III. fcc LATTICE

For the fcc lattice, the ordering is expected to be much more complicated by the analogy with the antiferromagnetic Ising model. To describe the possible ordered structures it is wise to separate the density ($s_i^2$) and magnetic ($s_i$) degrees of freedom for the site $i$ on each of the four sublattices $a$, $b$, $c$, and $d$. If we neglect for the moment being the magnetic part, the ordered antiquadrupolar structures, which occur at low temperature for negative $K$ and consist of zero and nonzero spins, are those of the Cu-Au type binary alloys on the fcc lattice with nearest-neighbor interactions:[25] $L1_2$ (with stoichiometry $A_3B$), $L1_0$ ($AB$), $L1_2$ ($AB_3$), depending on the value of $\Delta$. In the BEG model $A$ corresponds to $s^2 = 0$ and $B$ to $s^2 = 1$. Thus, the concentrations $q = (q_a + q_b + q_c + q_d)/4$ of the stoichiometric phases are $\frac{1}{4}$, $\frac{1}{2}$, and $\frac{3}{4}$, respectively. The magnetic coupling $J$ then introduces additional ordering or up-down symmetry breaking on top of these structures.

That is, the magnetic coupling further splits these phases (including the disordered one) into regions with different magnetic order. There is *no* mapping between $J > 0$ and $J < 0$ for the fcc lattice, and therefore these cases should be treated separately. Below we define the phases, which appear in phase diagrams for $J > 0$: (1) Paramagnetic (P) $m_a = m_b = m_c = m_d = 0$, $q_a = q_b = q_c = q_d$, (2) ferromagnetic (F) $m_a = m_b = m_c = m_d \neq 0$, $q_a = q_b = q_c = q_d$, (3) paramagnetic $A_3B$ ($P_{31}$) $m_\alpha = 0$ for $\alpha = a, b, c, d$, $q_a = q_b = q_c < q_d$, (4) ferrimagnetic $A_3B$ ($I_{31}$) $0 < m_a = m_b = m_c < m_d$, $q_a = q_b = q_c < q_d$, (5) paramagnetic $AB$ ($P_{11}$) $m_\alpha = 0$ for $\alpha = a, b, c, d$, $q_a = q_b > q_c = q_d$, (6) ferrimagnetic $AB$ ($I_{11}$) $m_a = m_b > m_c = m_d > 0$, $q_a = q_b > q_c = q_d$, (7) paramagnetic $AB_3$ ($P_{13}$) $m_\alpha = 0$ for $\alpha = a, b, c, d$, $q_a = q_b = q_c > q_d$, (8) ferrimagnetic $AB_3$ ($I_{13}$) $m_a = m_b = m_c > m_d > 0$, $q_a = q_b = q_c > q_d$. Here we allow for permutations of the sublattices. All the phases defined above are either uniform or consist of *two* nonequivalent sublattices. These sublattices in turn consist of one to three of the original sc sublattices $a$, $b$, $c$, and $d$.

For $J < 0$, the phases are not limited to the two-sublattice ordering and the above notation is therefore not sufficient. The antiferromagnetic coupling causes additional ordering rather than symmetry breaking, which increases the number of nonequivalent sublattices up to four. In the case where the number of sublattices with different values of $q_\alpha$ is larger than two, we will use the number of sublattices as notation instead of the usual $A_xB_y$ formula. Thus, the additional phases appearing in the phase diagram for $J < 0$ are (9) antiferromagnetic $L1_0$ (AF) $m_a = m_b = -m_c = -m_d \neq 0$, $q_a = q_b = q_c = q_d$, (10) ferrimagnetic $A_3B$ ($I'_{31}$) $m_a = m_b = m_c \lesseqgtr 0$, $m_d \gtreqless 0$, $q_a = q_b = q_c < q_d$, (11) antiferromagnetic $AB$ ($AF_{11}$) $m_a = -m_b \neq 0$, $m_c = m_d = 0$, $q_a = q_b > q_c = q_d$, (12) three-sublattice ferrimagnetic ($I_3$) $-m_a > m_b = m_c > m_d > 0$, $q_a > q_b = q_c > q_d$, (13) three-sublattice ferrimagnetic ($I'_3$) $-m_a > m_b > m_c = m_d > 0$, $q_a > q_b > q_c = q_d$, (14) four-sublattice antiferromagnetic ($AF_4$) $-m_a = m_b \neq 0$, $m_c = m_d = 0$, $q_a = q_b > q_c > q_d$, (15) four-sublattice ferrimagnetic ($I_4$) $m_\alpha \neq m_\beta$, $q_\alpha \neq q_\beta$ for $\alpha \neq \beta$.

Again from a ground-state analysis it can be derived that at $T = 0$ and $J > 0$ the ordered phases F, P, $P_{31}$, $I_{11}$, and $I_{13}$ are separated in cyclic order by straight lines in the space ($K$, $\Delta$):

$$\begin{aligned} \Delta &= 6(K+1), \\ \Delta &= 0, \\ \Delta &= 4(K+1), \\ \Delta &= 8(K+1), \\ \Delta &= 12(K+1), \end{aligned} \tag{7}$$

which all meet at $K = -1$, $\Delta = 0$.

For $J < 0$ the $T = 0$ phase diagram in the coordinates ($K$, $\Delta$) is more complicated and we present it in Fig. 3. The CVM calculations of the finite temperature phase diagram on the fcc lattice were carried out within the tetrahedron-octahedron (TO) approximation.[25] The free-energy expansion for the uniform phase is

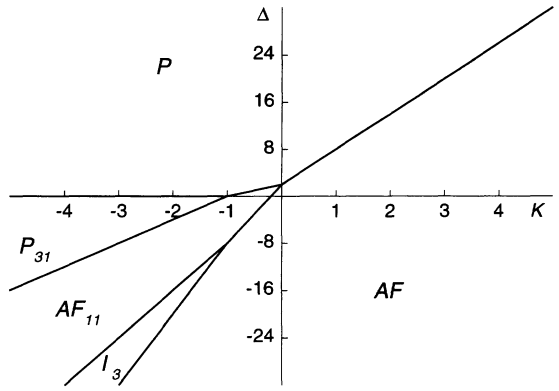


FIG. 3. Ground-state phase diagram ($K, \Delta$) of the BEG model on the fcc lattice for $J < 0$.

$$F = F_6 + 2F_4 - 8F_3 + 6F_2 - F_1, \tag{8}$$

where $F_6$, $F_4$, $F_3$, $F_2$, and $F_1$ are the free energies of the octahedron, tetrahedron, triangle, nearest-neighbor pair, and single-site clusters, respectively. In the general case of four-sublattice ordering the expansion includes four types of octahedra, triangles, and single-site clusters and six types of nearest-neighbor pairs.

The $J > 0$ case should be quite well described by the MFA results in the range $K > -1$, where no multisublattice ordering occurs, due to the large coordination of the fcc lattice. Instead we focus our attention on the $K < -1$ region by investigating two sections of the total phase diagram, at $K = -3$ and $K = -9$, which are quite representative, though this by no means is a complete account of all possible topologies of the phase diagram.

The phase diagrams are presented in Fig. 4. The familiar pattern of the phase diagram for a binary alloy on the fcc lattice with NN repulsive coupling, consisting of three ordered phases–$A_3B$, $AB$, and $AB_3$ (Ref. 25) is modified by the ferromagnetic ordering at higher concentration of non-zero spins, yielding the ferrimagnetic phases $I_{31}$, $I_{11}$, and $I_{13}$. The maximum temperatures of the ordered phases are reduced by the ferromagnetic ordering compared to those of the pure lattice gas model. Thus, for $K = -3$, the values of $T_{\max}/K$ are 0.407, 0.301, and 0.313, respectively, to be compared with 0.47, 0.45, and 0.47 for the lattice gas model (here the temperature is normalized by $K$, since it is the coupling constant for the pure lattice gas model with $J = 0$). Note, that for the $P_{31}$ phase the value of $T_{\max}$ is reduced by the ferromagnetic coupling even if there is no ferromagnetic ordering at that point (what one certainly should expect). Here we also mention that for $J < 0$ the antiferromagnetic coupling, in contrast to the case $J > 0$, increases $T_{\max}$ for the $AB$ phase, while $T_{\max}$ still decreases for the $A_3B$ phase and remains virtually unchanged for the $AB_3$ phase. We will not return to this matter further, more specifically the question of the interplay between the magnetic and chemical ordering of the fcc binary alloys with magnetic components has been investigated elsewhere.[26]

The critical line between the P and F phases is interrupted by a critical end point at the first-order line

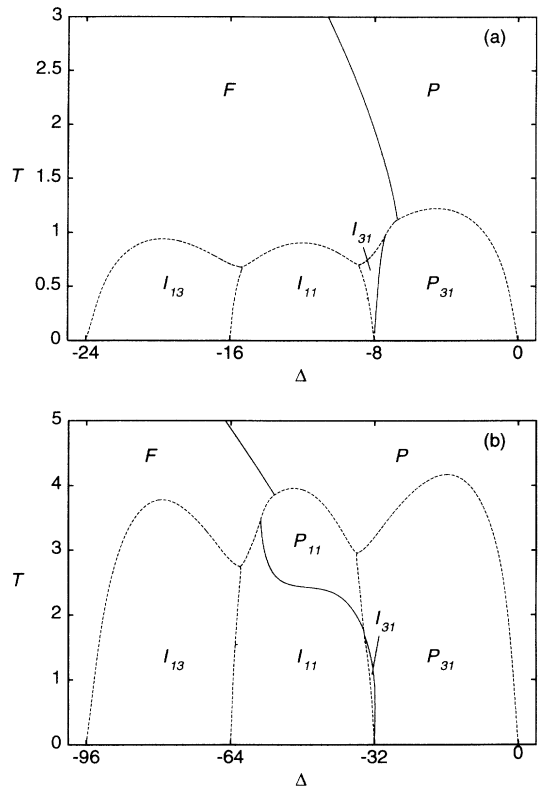


FIG. 4. Calculated $(T, \Delta)$ phase diagram of the BEG model on the fcc lattice at (a) $K = -3$, (b) $K = -9$, and $J > 0$.

between P and $P_{31}$ and then continues at lower $\Delta$ as the critical line between the paramagnetic and ferrimagnetic $A_3B$ phases ($P_{31}$ and $I_{31}$). The $\Delta$ gap on this line is obviously due to the jump of the nonzero spin concentration at the first-order line.

In general, the ferromagnetic ordering of the BEG model can be considered as that of a spin-$\frac{1}{2}$ Ising model on the dilute lattice produced by the antiquadrupolar ordering (or disorder), keeping in mind the fact that the ferromagnetic and antiquadrupolar interactions $J$ and $K$ are not independent. The phase diagram at $K = -9$ [Fig. 4(b)] is a suggestive manifestation of this interpretation. The higher-$\Delta$ part of the diagram is dominated by the antiquadrupolar ordering and the paramagnetic $AB$ phase ($P_{11}$) appears due to a reduced $J/K$ ratio. The critical line between the $P_{11}$ and $I_{11}$ phases exhibits a plateau, which is a result of layered antiquadrupolar $AB$ ordering. As the ordering is nearly perfect in the middle of the $AB$ phase for temperatures well below $T_{\max}$, the high-$q$ layers actually represent the square ferromagnetic spin-$\frac{1}{2}$ Ising model on the square lattice with a well defined $T_c$. The TO approximation is equivalent to the "square" approximation of the CVM, when only this layer is considered with $T_c = 2.426$.[27] At $\Delta = -48$ we obtain $T_c = 2.435$. The latter value should approach the former one as $|K/J| \to \infty$.

The existence of a narrow ferrimagnetic $A_3B$ phase close to the phase separation line between the $A_3B$ and $AB$ antiquadrupolar structures is also easily understood. Although the stoichiometric $A_3B$ phase at $q = 1/4$ does not show ferromagnetic ordering, the increase of $q$, when $\Delta$ is decreased, leads to an instability against magnetic ordering before the phase transition to the $AB$ structure occurs. As the critical concentration $q_c$ does not depend on $K$ at low temperature, the $I_{31}$ phase will appear in the phase diagram for any $K < -1$.

Further we can predict that, for even lower $K$, the maximum temperatures of the antiquadrupolar phases will increase with $|K|$, while the temperatures of ferromagnetic ordering remain stable. Consequently, the paramagnetic $AB_3$ phase ($P_{13}$) will appear, and yet another "plateau" of the critical line between $P_{13}$ and $I_{13}$ will correspond to the ferromagnetic ordering of an Ising model on the lattice consisting of three sc sublattices of the original fcc lattice.

The critical line between the P and F phase always saturates in the limit $q \to 1$ (large negative $\Delta$) at $T_c/12 = 0.834$, corresponding to the critical temperature of the Ising model on the fcc lattice in the TO approximation.[28]

We have not obtained the three-sublattice structures inside the $AB$ phase which were reported for the lattice gas model also from the TO approximation of the CVM.[29] Instead at $T/K \simeq 0.15$ we have found short first-order lines going from the boundaries towards the body of the AB phase. These lines are terminated by critical points inside the ordered phase.

For $J < 0$ the superposition of the antiferromagnetic and antiquadrupolar ordering appears to be much more complicated and not at all straightforward. We have made only one calculation at $K = -3$ and obtained the phase diagram (Fig. 5), featuring a total of 12 phases. The choice was made in order to cover the locus $K = -3$, $\Delta = -24$ where the BEG model again reduces to the antiferromagnetic Potts model [Eq. (5)]. In the lowest-$\Delta$ limit, the model is equivalent to the antiferromagnetic Ising model at zero field having a first-order phase transition to the $L1_0$ AF phase at $T_c = 1.809$ in TO approximation.[25] In the lowest-$K$ limit the $AB$

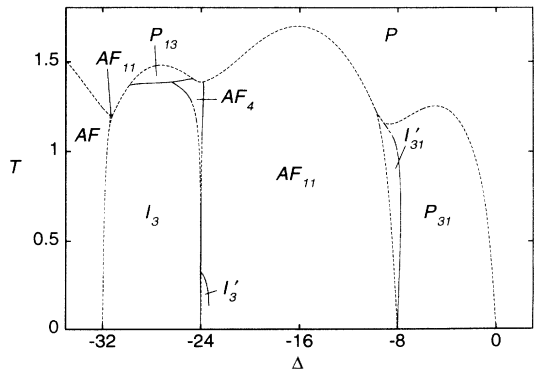


FIG. 5. Calculated $(T, \Delta)$ phase diagram of the BEG model on the fcc lattice at $K = -3$, $J < 0$. The solid line between phases $I_3$ and $AF_4$ is not a second-order line, since the second-order transition is symmetry forbidden. Instead, there are two second-order lines with a very narrow $I_4$ phase in between. It cannot be distinguished in this picture.

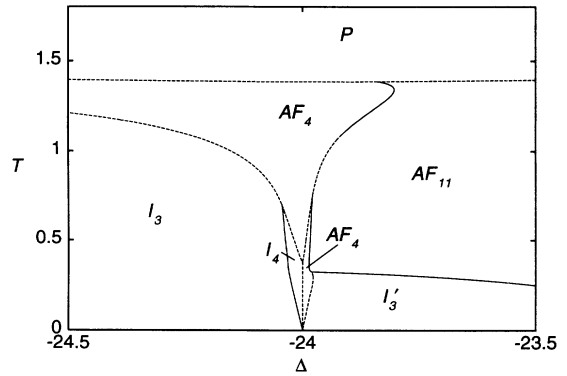


FIG. 6. Enlarged part of Fig. 5 in the vicinity of $\Delta = -24$. The two $AF_4$ phases have the same symmetry but are quantitatively different at their coexistence line

phase is also expected to be split into paramagnetic $P_{11}$ and antiferromagnetic $AF_{11}$ phases by a critical line with a plateau at $T_c = 2.426$.

The enlarged part of the phase diagram near $\Delta = -24$ is presented in Fig. 6. In contrast to what we have found for the sc lattice, the line of the Potts model is not a first-order phase-coexistence line from the Potts transition at $T_{c1} = 1.387$ down to $T_{c2} = 0.379$. The value of the Potts transition temperature is by 8% above the result of the MC estimate: $T_{c1} = 1.28 \pm 0.04$.[30] The temperature dependence of the Potts state probabilities $p_i^\alpha$, $i = 1,2,3$, $\alpha = a,b,c,d$ are presented in Fig. 7. The ordered phase between $T_{c1}$ and $T_{c2}$ has three sublattices mainly occupied by one of the three different states each, while the fourth sublattice is occupied by all the states at random with one-third probability, e.g., $p_2^a = p_3^b = p_1^c = p_{\rm high} > \frac{1}{3}$, $p_1^a = p_3^a = p_1^b = p_2^b = p_2^c = p_3^c = p_{\rm low} < \frac{1}{3}$, $p_1^d = p_2^d = p_3^d = \frac{1}{3}$. This phase is 24-fold degenerate, what is matched by the same degeneracy of the $AF_4$ phase. The simple extrapolation of this phase down to $T = 0$ would suggest perfect ordering on three sublattices with the complete disorder on the fourth with the residual entropy $s = \frac{1}{4}\ln 3 = 0.2747$ which is a lower bound for the actual entropy. From the analogy with the ordering on the sc lattice, one could expect saturation

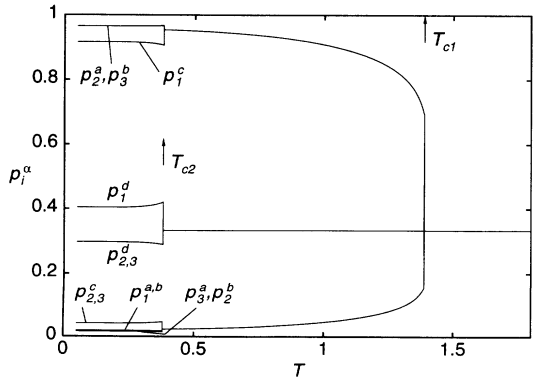


FIG. 7. The temperature dependence of the expectation values for different states of the AF Potts model on the fcc lattice, corresponding to $J < 0$, $K = -3$, and $\Delta = -24$.

of $p_{\rm high}$ below 1 and $p_{\rm low}$ above 0 with somewhat larger residual entropy due to the possibility of the Potts state being on the "wrong" lattice if it is permitted by the nearest neighbors. In our CVM calculations, by formally extending this phase down to $T = 0$, we would obtain $p_{\rm high} = 0.9559$, $p_{\rm low} = 0.0221$, and $s = 0.2987$.

However below $T_{c2}$ a first-order line between the $I_4$ and $AF_4$ phases appears, indicating a change of the ordering along the $\Delta = -24$ line. Again we have found an additional first-order phase transition inside the ordered phase of the antiferromagnetic Potts model. The ordering below $T_{c2}$ is described by the following expectations of the Potts states: $p_2^a = p_3^b > p_1^c > p_1^d > \frac{1}{3}$, $p_3^a = p_2^b < p_1^a = p_1^b < p_2^c = p_3^c < p_2^d = p_3^d < \frac{1}{3}$. There are 72 nonequivalent permutations of the sublattices and Potts states for the latter phase, which are realized via the coexistence of the 48-fold degenerate $I_4$ phase and 24-fold degenerate $AF_4$ phase. The residual entropy per site at $T = 0$ is finite due to the frustration of the ground state — we obtain $s = 0.2991$.

## IV. SUMMARY

The phase diagram of the BEG model on the simple-cubic lattice was calculated by means of the CVM within the eight-point cubic cluster approximation. Although most features of the phase diagram are qualitatively similar to the previous MFA results, quantitatively the results are much closer to the MC data, where these are available. Near the locus $K = -3$, $\Delta = -12$, where the BEG model reduces to the three-state antiferromagnetic Potts model, we have obtained rather unexpected results. In this region we obtained *two* ferrimagnetic phases, one on either side of the $\Delta = -12$ line, instead of one predicted by the MFA, and a third ferrimagnetic phase emerges at $K < -3$. This implies the existence of additional phase transitions in the ordered phase of the three-state antiferromagnetic Potts model. Actually we have found two transitions of the first and second order, respectively. These transitions control the changes in the ordering regime of the three states on the two sublattices. The phase diagrams of the BEG model on the face-centered cubic lattice were obtained for the first time for $K < -1$ and both for ferromagnetic ($J > 0$) and antiferromagnetic ($J < 0$) coupling, featuring a number of new phases, due to the interplay of the magnetic and quadrupolar ordering. Another first-order phase transition is also predicted inside the ordered phase of the antiferromagnetic Potts model on the fcc lattice. These results are supposed to describe classical systems, where both symmetry-breaking and density fluctuations are important, such as binary alloys with magnetic components.

## ACKNOWLEDGMENTS

This work was supported by The Swedish Natural Science Research Council, The Swedish Institute, The Knut and Alice Wallenberg Foundation, and The Göran Gustafsson Foundation.

* Permanent address: Faculty of Physics, Vilnius University, Saulėtekio 9, 2054 Vilnius, Lithuania.

[1] M. Blume, V. J. Emery, and R. B. Griffiths, Phys. Rev. A **4**, 1071 (1971).
[2] D. Furman, S. Dattagupta, and R. B. Griffiths, Phys. Rev. B **15**, 441 (1977).
[3] J. Lajzerowicz and J. Sivardière, Phys. Rev. A **11**, 2079 (1975); J. Sivardière and J. Lajzerowicz, *ibid.* **11**, 2090 (1975); **11**, 2101 (1975).
[4] D. Mukamel and M. Blume, Phys. Rev. A **10**, 619 (1974).
[5] A. N. Berker and M. Wortis, Phys. Rev. B **14**, 4946 (1976); M. Kaufman, R. B. Griffiths, J. M. Yeomans, and M. E. Fisher, *ibid.* **23**, 3448 (1981); Th. W. Burkhardt, *ibid.* **14**, 1196 (1976).
[6] D. M. Saul, M. Wortis, and D. Stauffer, Phys. Rev. B **9**, 4964 (1974).
[7] B. L. Arora and D. P. Landau, *Proceedings of the 18th Annual Conference on Magnetism and Magnetic Materials* AIP Conf. Proc. No. 10, edited by C. D. Graham and J. J. Rhyne (AIP, New York, 1972), p. 870.
[8] M. Tanaka and T. Kawabe, J. Phys. Soc. Jpn. **54**, 2194 (1985).
[9] Y. L. Wang and C. Wentworth, J. Appl. Phys. **61**, 4411 (1987).
[10] Y. L. Wang, F. Lee, and J. D. Kimel, Phys. Rev. B **36**, 8945 (1987).
[11] T. Horiguchi, Phys. Lett. **113A**, 425 (1986).
[12] F. Y. Wu, Phys. Lett. A **116**, 245 (1986).
[13] A. Rosengren and R. Häggkvist, Phys. Rev. Lett. **63**, 660 (1989).
[14] L. H. Gwa and F. Y. Wu, Phys. Rev. B **43**, 13755 (1991).
[15] R. R. Netz and A. N. Berker, Phys. Rev. B **47**, 15019 (1993).
[16] A. Bakchich, A. Benyoussef, and M. Touzani, Physica A **186**, 524 (1992).
[17] A. Rosengren and S. Lapinskas, Phys. Rev. B **47**, 2643 (1993).
[18] V. Talanquer, C. Varea, and A. Robledo, Phys. Rev. B **39**, 7030 (1989).
[19] W. Hoston and A. N. Berker, Phys. Rev. Lett. **67**, 1027 (1991).
[20] W. Hoston and A. N. Berker, J. Appl. Phys. **70**, 6101 (1991).
[21] R. R. Netz, Europhys. Lett. **17**, 373 (1992).
[22] K. Kasono and I. Ono, Z. Phys. B **88**, 205 (1992).
[23] A. Rosengren and S. Lapinskas, Phys. Rev. Lett. **71**, 165 (1993).
[24] Y. Ueno, G. Sun, and I. Ono, J. Phys. Soc. Jpn. **58**, 1162 (1989).
[25] J. M. Sanchez, D. de Fontaine, and W. Teitler, Phys. Rev. B **26**, 1465 (1982).
[26] J. M. Sanchez and C. H. Lin, Phys. Rev. B **30**, 1448 (1984).
[27] R. Kikuchi, Phys. Rev. **81**, 988 (1951).
[28] S. K. Aggarwal and T. Tanaka, Phys. Rev. B **16**, 3963 (1977).
[29] A. Finel and F. Ducastelle, Europhys. Lett. **1**, 135 (1986); **1**, 543E (1986).
[30] G. S. Grest, J. Phys. A **14**, L217 (1981).